

Theory of carrier transport in graphene double-layer structure with carrier imbalance

Kazuhiro Hosono and Katsunori Wakabayashi

International Center for Materials Nanoarchitectonics (WPI-MANA), National Institute for Materials Science (NIMS), Tsukuba, Ibaraki, 305-0044, Japan

The carrier mobility of a graphene double-layer system is evaluated on the basis of the Boltzmann transport theory. In this system, two graphene layers are separated by a dielectric barrier layer. We focus on the cases in which there is carrier imbalance between the two layers. It is found that the mobility can be improved by controlling the carrier density polarization between the two layers if we choose an appropriate dielectric environment.

1. Introduction

Graphene, a one atomic-thickness carbon sheet, has attracted much interest owing to its unique electronic properties such as the half-integer Hall effect and ultra-high mobility. The electronic states of graphene near the Fermi energy are well described by the two-dimensional massless Dirac equation.

Recently, electronic devices composed of graphene and other atomically thin materials have also been proposed¹⁻⁵⁾. One such system is the graphene double-layer system, in which two graphene layers are separated by a thin dielectric, as shown in Fig. 1(a)²⁻⁸⁾. Since the interlayer interaction can be controlled by adjusting the interlayer distance, the GDLS has been considered to be a good platform for studying the exciton superfluidity⁹⁻¹¹⁾, Coulomb drag effect^{10,12)} and plasmon mode¹³⁻¹⁵⁾. The Coulomb drag effect was demonstrated using Al_2O_3 ²⁾ and h-BN^{3,4,16-18)} as middle dielectrics. Theoretical analysis of the device performance of GDLS has only just begun.

Carrier mobility is one of the key benchmarks of device performance because it determines the power dissipation and switching speed of the device. Recent theory suggests improving carrier mobility by placing a high- κ overlayer on a semiconductor nanostructure, which leads to the weakening of Coulomb scattering due to the screening effect^{19,20)}. Indeed, several electronic transport measurements of graphene or atomically-thin material have successfully revealed mobility enhancement via change in the

dielectric environment^{21–25}). In our previous paper, we have constructed a formulation for evaluating the dependence of the interlayer distance and the effect of the dielectric environment on the charged-impurity-limited carrier mobility of the GDLS on the basis of the Boltzmann transport theory.

We have pointed out that the carrier mobility of GDLS strongly depends on the dielectric constant of the barrier layer when the interlayer distance becomes larger than the inverse of the Fermi wave vector²⁶). However, we have considered only the case in which the carrier concentrations at each layer are equivalent ($n_c^{(1)} = n_c^{(2)}$), and have neglected carrier density polarization, for simplicity. Since the carrier density at each layer can be controlled by adjusting the gate voltage in the experiments, it is necessary to develop a theory that takes carrier imbalance into account.

In this study, we focus on the case in which there is carrier imbalance. We evaluate the effect of carrier density polarization (denoted by Δn_c) on the charged-impurity-limited carrier mobility in the GDLS by extending our previously -reported formulation. It is found that the carrier density polarization dependence of the carrier mobility is affected by the surrounding dielectrics and interlayer distance. The carrier mobility in the presence of carrier density imbalance strongly depends on the interlayer distance if we set particular constants of the dielectric environment. Our result offers appropriate ranges of the carrier polarization and dielectric constant of the surrounding dielectrics to improve the charged-impurity limited mobility of GDLS.

2. Model and formulation

Figure 1(a) shows a schematic of the GDLS, in which two graphene layers are separated by three different dielectrics, i.e., ϵ_1, ϵ_2 and ϵ_3 . We assume that the two graphene layers are coupled only through the Coulomb interaction between the charged impurities and carriers. The Hamiltonian can be written as

$$H = \gamma \sum_{\mathbf{k}, s, s'} \sum_{i=1}^2 c_{\mathbf{k}, s, i}^\dagger (\sigma_x k_x + \sigma_y k_y) c_{\mathbf{k}, s', i} \quad (1)$$

$$+ \frac{1}{L^2} \sum_{\mathbf{k}, \mathbf{q}} \sum_{s, s'} \sum_{i, j} W_{ij}(\mathbf{q}, d) c_{\mathbf{k}+\mathbf{q}, s, i}^\dagger c_{\mathbf{k}, s', i} \rho_{\text{imp}}^{(j)}(\mathbf{q}),$$

where $c_{\mathbf{k}, s, i}^\dagger$ ($c_{\mathbf{k}, s, i}$) is the creation (annihilation) operator for an electron with the wave vector $\mathbf{k} = (k_x, k_y)$ and the pseudospin s on the i -th graphene layer. Here, $\gamma = 6.46 \text{ eV} \cdot \text{\AA}$ is the band parameter. σ_x and σ_y are the Pauli spin matrices for pseudospin; $s, s' = \pm 1$ are pseudospin labels for describing the sublattice of the honeycomb lattice. L^2 is the

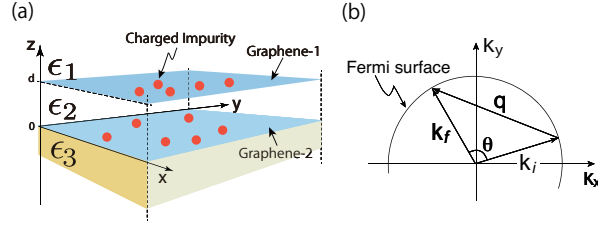


Fig. 1. (a) Schematic of GDLS with three different dielectrics. The interlayer distance between two graphene layers is defined as d . The dielectrics with ϵ_1 and ϵ_3 are assumed to be much thicker than the interlayer distance d . The top and bottom graphene layers are numbered 1 and 2, respectively. The red circles represent randomly distributed charged impurities. (b) Carrier scattering on a Fermi surface of radius k_F . An initial state with a wave vector \mathbf{k}_i is scattered by a charged impurity potential to a final state with a wavevector \mathbf{k}_f , where $|\mathbf{k}_i| = |\mathbf{k}_f| = k_F$. Here $\mathbf{q} = \mathbf{k}_f - \mathbf{k}_i$, and θ is the scattering angle.

area of each graphene layer. W_{ij} denotes the Fourier component of the screened Coulomb potential, which depends on the interlayer distance d , and includes the effect of the Coulomb interaction between carriers on each graphene layer through the polarization function³³⁾. $\rho_{\text{imp}}^{(j)}(\mathbf{q}) = \sum_{\alpha}^{N_{\text{imp}}} e^{-i\mathbf{q}\cdot\mathbf{R}_{\alpha}^{(j)}}$ is the particle density of random impurities on the j -th graphene layer having the total number of impurities N_{imp} . $\mathbf{R}_{\alpha}^{(j)}$ represents the position of the impurities on the j -th layer. The inverse of the carrier mobility μ^{-1} can be described by $\mu^{-1} = \mu_{11}^{-1} + \mu_{22}^{-1} + \mu_{12}^{-1} + \mu_{21}^{-1}$ ^{28,29)}. Here, μ_{11}^{-1} (μ_{22}^{-1}) is the contribution of the intralayer scattering rate of the first (second) graphene layer, and μ_{12}^{-1} and μ_{21}^{-1} are the contributions of interlayer scattering. According to the semiclassical Boltzmann theory, the inverse of the each contribution of carrier mobility is given by

$$\frac{1}{\mu_{ij}(k_i)} = \frac{n_{ij}^{\text{imp}} \sqrt{n_c^{(i)}} \pi}{e\gamma} D(k_i) \int_0^{\pi} d\theta |W_{ij}(q_i, d)|^2 (1 - \cos^2 \theta), \quad (2)$$

where n_{11}^{imp} (n_{22}^{imp}) is the impurity concentration on the first (second) graphene layer. The impurity concentration for interlayer scattering is given as the average of two layers $n_{12}^{\text{imp}} \equiv (n_{11}^{\text{imp}} + n_{22}^{\text{imp}})/2$. For simplicity, we assume that the impurity concentration at each layer $n_i = n_{11}^{\text{imp}} = n_{22}^{\text{imp}}$ is equivalent and that the Fermi level of both graphene layers lies in the conduction band. $D(k_i) = gk_i/2\pi\gamma$ is the density of states of single-layer graphene with $g = 4$ owing to the valley and spin degeneracy. θ is the scattering angle, and $q_i = 2k_{F,i} \sin(\theta/2)$ is the scattering wave vector on the circular two-dimensional Fermi surface, as shown in Fig. 1(b). The Fermi wave number on each graphene layer is given as $k_{F,i} = \sqrt{4\pi n_c^{(i)}/g}$. Note that the last θ -dependent factor also contains the phase of the wave function of graphene^{29,33)}. The structural parameter such as the

interlayer distance d and scattering potential due to charged impurities are included in the screened potentials W_{ij} .

Here, we briefly explain the derivation of the screened Coulomb potential W_{ij} from the unscreened one v_{ij} . The analytical expression of the unscreened Coulomb potentials of the GDLS can be derived using the image charge method^{19,25,27)}. For this system, we need to consider an infinite series of point image charges arising from two interfaces at $z = 0$ and d shown in Fig. 1(a), where two types of dielectrics are spanned by a graphene layer. The resulting unscreened Coulomb potentials are given as

$$v_{11}(q_1, d) = \frac{4\pi e^2}{q_1} \frac{\epsilon_2 + \epsilon_3 \tanh(q_1 d)}{X_1}, \quad (3)$$

$$v_{22}(q_2, d) = \frac{4\pi e^2}{q_2} \frac{\epsilon_2 + \epsilon_1 \tanh(q_2 d)}{X_2}, \quad (4)$$

$$v_{12}(q_1, d) = \frac{4\pi e^2}{q_1} \frac{\epsilon_2}{X_1 \cosh(q_1 d)}, \quad (5)$$

$$v_{21}(q_2, d) = \frac{4\pi e^2}{q_2} \frac{\epsilon_2}{X_2 \cosh(q_2 d)}. \quad (6)$$

Here v_{11} and v_{22} are the intralayer Coulomb interactions on the first and second graphene layers, respectively. v_{12} and v_{21} are the interlayer Coulomb interactions, and we define

$$X_i = \epsilon_2(\epsilon_1 + \epsilon_3) + (\epsilon_2^2 + \epsilon_1\epsilon_3) \tanh(q_i d). \quad (7)$$

The above potentials have been used in the context of the superfluid magnetoexcitons⁹⁾ and plasmon mode^{14,15)} of the GDLS. The above expressions indicate that the parameter $q_i d$ ($\approx k_F d$) determines the screening behavior and the strength of the interlayer Coulomb interaction.

The screened Coulomb potentials are described by the random phase approximation (RPA) as

$$W = V + V\Pi W = V(1 - V\Pi)^{-1}, \quad (8)$$

where

$$V = \begin{pmatrix} v_{11} & v_{12} \\ v_{21} & v_{22} \end{pmatrix},$$

$$\Pi = \begin{pmatrix} \Pi_1 & 0 \\ 0 & \Pi_2 \end{pmatrix}.$$

Here, $\Pi_1(\Pi_2)$ is the static polarization function of the first (second) graphene layer

^{28,29)}. The static polarization is written as

$$\Pi_i = \Pi_i^{(+)} + \Pi_i^{(-)}, \quad (9)$$

where $\Pi_i^{(+)}$ and $\Pi_i^{(-)}$ are given as

$$\Pi_i^{(+)} = \begin{cases} D(k_{F,i}) \left(1 - \frac{\pi}{4} \frac{q_i}{2k_{F,i}}\right) & (\frac{q_i}{2} \leq k_{F,i}) \\ D(k_{F,i}) \left(1 - \frac{1}{2} \sqrt{1 - 4\left(\frac{k_{F,i}}{q_i}\right)^2} - \frac{1}{4} \frac{q_i}{k_{F,i}} \arcsin\left(\frac{2k_{F,i}}{q_i}\right)\right) & (\frac{q_i}{2} > k_{F,i}), \end{cases}$$

$$\Pi_i^{(-)} = D(k_{F,i}) \frac{\pi}{8k_{F,i}} q_i. \quad (10)$$

From Eq. (8), the effective interactions are obtained as

$$W_{11} = \frac{1}{\varepsilon} (v_{11} + (v_{11}v_{22} - v_{12}v_{21})\Pi_2), \quad (11)$$

$$W_{22} = \frac{1}{\varepsilon} (v_{22} + (v_{11}v_{22} - v_{12}v_{21})\Pi_1), \quad (12)$$

$$W_{12} = \frac{v_{12}}{\varepsilon}, \quad (13)$$

$$W_{21} = \frac{v_{21}}{\varepsilon}. \quad (14)$$

where the intralayer interactions v_{11} and v_{22} , and the interlayer interactions v_{12} and v_{21} are defined in Eqs. (3)-(6), respectively. Here, the dielectric function is defined as

$$\varepsilon(q_1, q_2) = \det(1 - V\Pi) = (1 + v_{11}\Pi_1)(1 + v_{22}\Pi_2) - v_{12}v_{21}\Pi_1\Pi_2. \quad (15)$$

By combining Eqs. (11)-(15), we can evaluate the carrier mobility of GDLS in the presence of an imbalance in the concentration between two graphene layers, i.e., $n_c^{(1)} \neq n_c^{(2)}$.

3. Results and discussion

We first investigated the dependence of the dielectric function Eq. (15) on the interlayer distance d and carrier density polarization. Here, we define the carrier density polarization as $\Delta n_c = (n_c^{(2)} - n_c^{(1)}) / (n_c^{(1)} + n_c^{(2)})$, and fix the total carrier concentration at $n_c^{(1)} + n_c^{(2)} = 2 \times 10^{12}/\text{cm}^2$. When the carriers are only in the first (second) layer, $\Delta n_c = -1(1)$. In the case of $\Delta n_c = 0$ in which the two layers have identical carrier densities, the dielectric function captures the screening effect of scattering potentials due to charged impurities. In order to see the role of the middle dielectric layer, we assume the dielectric constants for the top and bottom layers as $\epsilon_1 = \epsilon_{\text{Air}} = 1$ and $\epsilon_3 = \epsilon_{\text{Al}_2\text{O}_3} = 12.53$, respectively, and consider three different dielectrics as the middle layer, i.e., h-BN, Al_2O_3 , and HfO_2 . Their dielectric constants are $\epsilon_{\text{h-BN}} = 4$,

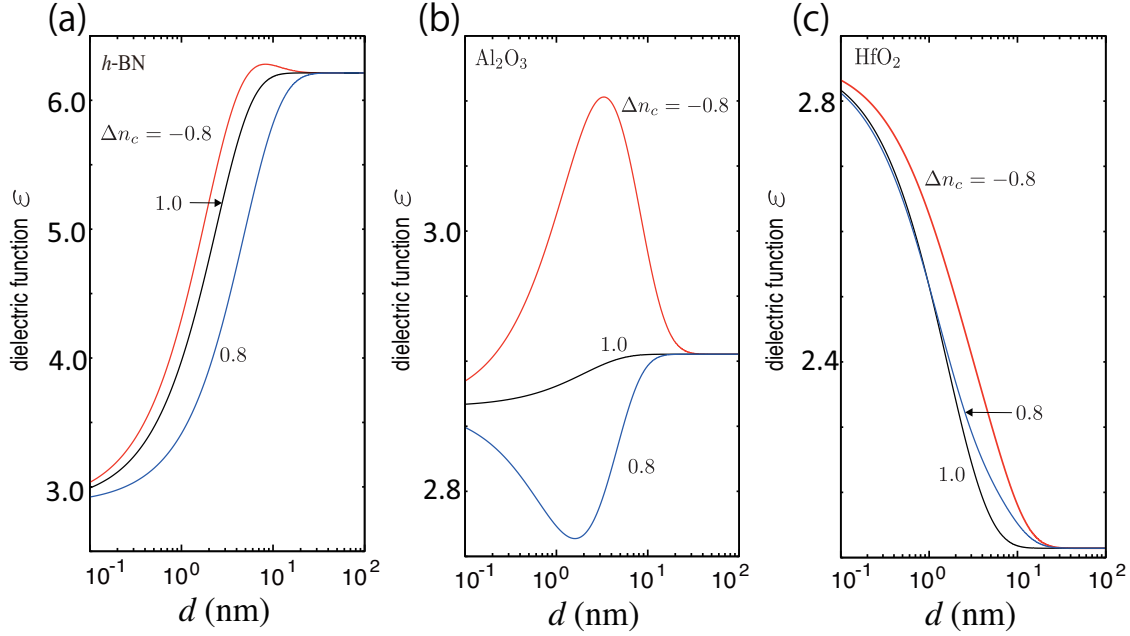


Fig. 2. Interlayer distance d dependence of the dielectric function at the scattering angle $\theta = \pi/2$ for three different density polarizations $\Delta n_c = -0.8, 1$ and 0.8 . Left, middle, and right panels represent the cases of h-BN, Al_2O_3 and HfO_2 , respectively. Here the total carrier density is $n_c^{(1)} + n_c^{(2)} = 2 \times 10^{12}/\text{cm}^2$.

$\epsilon_{\text{Al}_2\text{O}_3} = 12.53$, and $\epsilon_{\text{HfO}_2} = 22$, respectively^{30–32}).

Figure 2 shows the d dependences of the dielectric function at a scattering angle $\theta = \pi/2$ for several different density polarizations, i.e., $\Delta n_c = -0.8, 1$, and 0.8 for three different middle dielectrics. Figures 2(a)–(c) represent the cases of h-BN, Al_2O_3 and HfO_2 , respectively. We can see that screening effect at $\theta = \pi/2$ is enhanced with increasing interlayer distance in the case of h-BN ($\epsilon_2 < \epsilon_3$), as shown in Fig. 2(a), but reduced for HfO_2 ($\epsilon_2 > \epsilon_3$), as shown in Fig. 2(c). We see that the Δn_c dependences in these two cases are weak, because of the large mismatch between ϵ_2 and ϵ_3 . However, for Al_2O_3 ($\epsilon_2 = \epsilon_3$), we can see that the presence of carrier polarization leads to very different behaviors of the interlayer distance as shown in Fig. 2(b), together with a peak structure $\Delta n_c = -0.8$. However, at $\Delta n_c = 0.8$, a dip appears instead. Since the d dependence of the dielectric screening effect in the case of $\epsilon_2 \simeq \epsilon_3$ is weaker than those in other cases, the effect of the carrier density polarization becomes prominent.

Figures 3(a)–(c) show the dependences of the total mobility at the interlayer distance d for two different carrier polarizations $\Delta n_c = -0.8$ and 0.8 in the same dielectric environment as in Figs. 2(a)–(c), respectively. These mobilities are strongly affected by

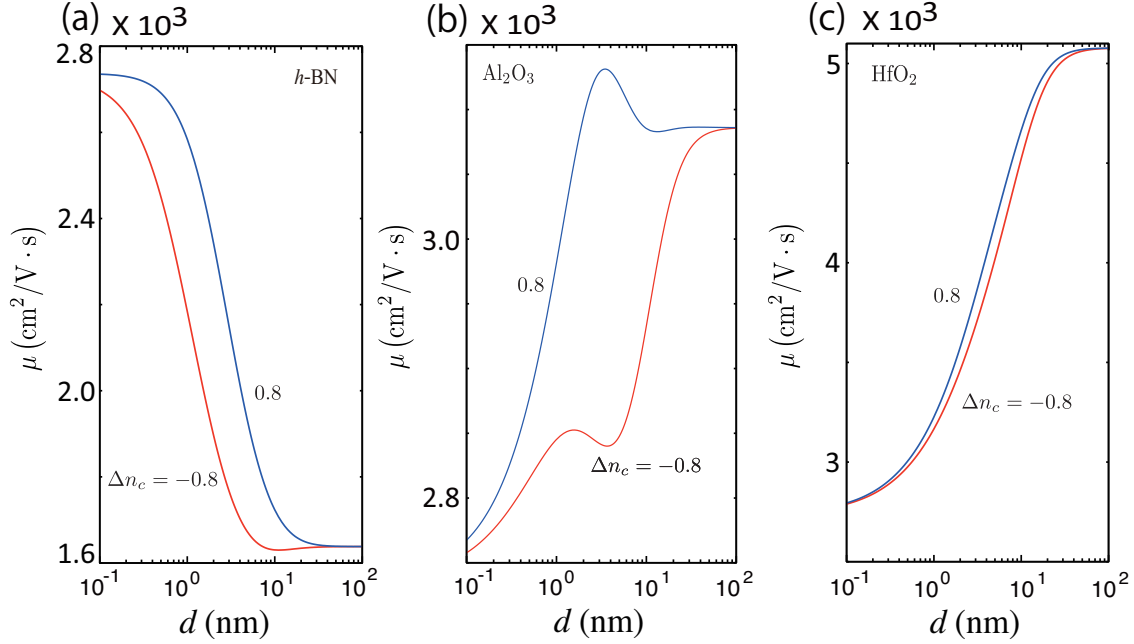


Fig. 3. (a) Plots of mobility versus interlayer distance for different carrier density polarizations, $\Delta n_c = -0.8, 0.8$. Here, the total carrier density is $n_c^{(1)} + n_c^{(2)} = 2 \times 10^{12}/\text{cm}^2$, the impurity density is $n_i^{(1)} = n_i^{(2)} = 5 \times 10^{11}/\text{cm}^2$, $\epsilon_1 = \epsilon_{\text{Air}} = 1$, and $\epsilon_2 = \epsilon_3 = \epsilon_{\text{Al}_2\text{O}_3} = 12.53$.

dielectric functions. In particular, when we choose Al_2O_3 as the middle dielectric, the mobility in Fig. 3(b) shows a dip for $\Delta n_c = -0.8$ and a peak for $\Delta n_c = 0.8$, arising from the peak or dip structure in the dielectric functions, as shown in Fig. 2(b).

We show, in Fig. 4, the d dependence of the four components of the inverse of the mobility at $\Delta n_c = -0.8$ (left) and 0.8 (right). By comparing the left and right panels in Fig. 4, we find that the interlayer components μ_{12} and μ_{21} are exchanged by changing the carrier polarization. The intralayer component μ_{11} is almost unaffected by the inversion of the carrier polarization, because the Δn_c dependence is canceled out in the effective potential W_{11} [Eq. (11)] for $\epsilon_1 \ll \epsilon_2, \epsilon_3$.

On the other hand, another intralayer component, μ_{22} , considerably depends on the interlayer distance d and carrier density polarization. The reason for this is that the Δn_c dependence of the dielectric function cannot be canceled out in the effective potential [Eq. (12)]. We found that the characteristic d and Δn_c dependences of the carrier mobility for $\epsilon_1 \ll \epsilon_2 \simeq \epsilon_3$ were dominated by one of the intralayer components, i.e., μ_{22} .

In summary, we have investigated the carrier transport of GDLS in the presence of carrier polarization by extending our previous theory. We showed that the carrier

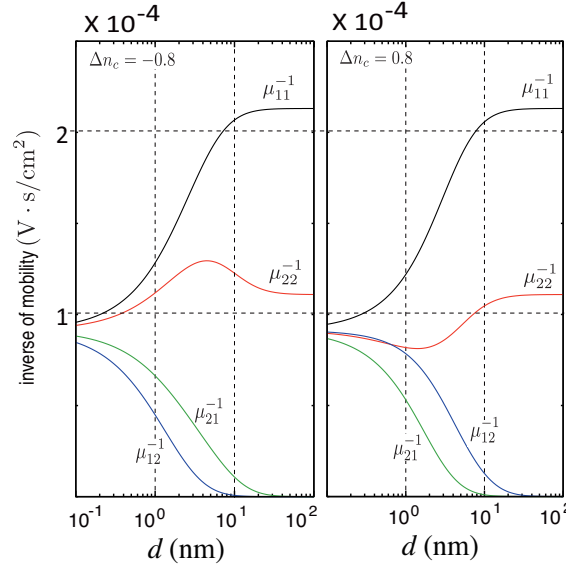


Fig. 4. Four components of the inverse of mobility as function of the interlayer distance for $\Delta n_c = -0.8$ (left) and $\Delta n_c = 0.8$ (right).

mobility considerably depends on the carrier density polarization when the dielectric environment parameters ϵ_1 , ϵ_2 , and ϵ_3 are satisfied under the condition $\epsilon_1 \ll \epsilon_2 \simeq \epsilon_3$. Our result reveals that the mobility can be improved by choosing higher-dielectric-constant materials as well as introducing the carrier polarization between two layers. From our results, we propose guidelines for experiments on and applications of new functional atomically thin devices.

Acknowledgment

This work is supported by Grants-in-Aid for Scientific Research (KAKENHI) (Nos. 25107005, 25107001, 224710153, and 23310083) from the Japan Society for the Promotion of Science.

References

- 1) K. S. Novoselov and A. H. Castro Neto: Phys. Scr. **T146** (2012) 014006.
- 2) S. Kim, I. Jo, J. Nah, Z. Yao, S. K. Banerjee, and E. Tutuc: Phys. Rev. B **83** (2011) 161401.
- 3) C. R. Dean, A. F. Young, I. Meric, C. Lee, L. Wang, S. Sorgenfre, K. Watanabe, T. Taniguchi, P. Kim, K. L. Shepard and J. Hon: Nat. Nanotechnol. **5** (2010) 722.
- 4) L. A. Ponomarenko, A. K. Geim, A. A. Zhukov, R. Jalil, S. V. Morozov, K. S. Novoselov, I. V. Grigorieva, E. H. Hill, V. V. Cheianov, V. I. Fal'ko, K. Watanabe, T. Taniguchi, and R. V. Gorbachev: Nat. Phys. **7** (2011) 958.
- 5) L. Britnell, R. M. Ribeiro, A. Eckmann, R. Jalil, B. D. Belle, A. Mishchenko, Y.-J. Kim, R. V. Gorbachev, T. Georgiou, S. V. Morozov, A. N. Grigorenko, A. K. Geim, C. Casiraghi, A. H. Castro Neto, and K. S. Novoselov: Science **340** (2013) 1311.
- 6) V. Ryzhii, T. Otsuji, M. Ryzhii, V. G. Leiman, S. O. Yurchenko, V. Mitin, and M. S. Shur: J. Appl. Phys. **112** (2012) 104507.
- 7) V. Ryzhii, A. A. Dubinov, T. Otsuji, V. Ya. Aleshkin, M. Ryzhii, and M. Shur: OPT EXPRESS **21** (2013) 25.
- 8) A. Ishikawa and T. Tanaka: Appl. Phys. Lett. **102** (2013) 253110.
- 9) A. A. Pikalov and D. V. Fil: Nanoscale Res. Lett. **7** (2012) 145.
- 10) M. P. Mink, H. T. C. Stoof, R. A. Duine, M. Polini, and G. Vignale: Phys. Rev. Lett. **108** (2012) 186402.
- 11) D. S. L. Abergel, M. Rodriguez-Vega, Enrico Rossi, and S. Das Sarma: Phys. Rev. B **88** (2013) 235402.
- 12) B. Scharf and A. Matos-Abiague: Phys. Rev. B **86** (2012) 115425.
- 13) T. Stauber and G. Gomez-Santos: Phys. Rev. B **85** (2012) 075410.
- 14) S. M. Badalyan and F. M. Peeters: Phys. Rev. B **85** (2012) 195444.
- 15) R. E. V. Profumo, R. Asgari, M. Polini, and A. H. MacDonald: Phys. Rev. B **85** (2012) 085443.
- 16) R. V. Gorbachev, A. K. Geim, M. I. Katsnelson, K. S. Novoselov, T. Tudorovskiy, I. V. Grigorieva, A. H. Macdonald, S. V. Morozov, K. Watanabe, T. Taniguchi, and L. A. Ponomarenko: Nat. Phys. **8** (2012) 896.
- 17) G. H. Lee, Y. J. Yu, C. Lee, C. Dean, K. L. Shepard, P. Kim, and J. Hone: Appl. Phys. Lett. **99** (2011) 243114.

- 18) P. J. Zomer, S. P. Dash, N. Tombros, and B. J. van Wees: Appl. Phys. Lett. **99** (2011) 232104.
- 19) D. Jena and A. Konar: Phys. Rev. Lett. **98** (2007) 136805.
- 20) S. Adam, E. H. Hwang, V. M. Glitski, and S. Das Sarma: Proc. Natl. Acad. Sci. U.S.A. **104** (2007) 1392.
- 21) C. Jang, S. Adam, J.-H. Chen, E. D. Williams, S. Das Sarma, and M. S. Fuhrer: Phys. Rev. Lett. **101** (2008) 146805.
- 22) S. Kim, J. Nah, I. Jo, D. Shahrjerdi, L. Colombo, Z. Yao, E. Tutuc, and S. K. Banerjee: Appl. Phys. Lett. **94** (2009) 062107.
- 23) B. Radisavljevic, M. B. Whitwick, and A. Kis: Nat. Nanotechnol. **6** (2011) 147.
- 24) M. J. Hollander, M. Labella, Z. R. Hughes, M. Zhu, K. A. Trumbull, R. Cavaleiro, D. W. Snyder, X. Wang, E. Hwang, S. Datta, and J. A. Robinson: Nano Lett. **11** (2011) 3601.
- 25) S.-L. Li, K. Wakabayashi, Y. Xu, S. Nakaharai, K. Komatsu, W.-W Li, Y.-F. Lin, A. Aparecido-Ferreira, and K. Tsukagoshi: Nano Lett **13** (2013) 3546.
- 26) K. Hosono and K. Wakabayashi: Appl. Phys. Lett. **103** (2013) 033102.
- 27) M. Kumagai and T. Takagahara: Phys. Rev. B **40** (1989) 12359.
- 28) T. Ando: J. Phys. Soc. Jpn. **75** (2006) 074716.
- 29) K. Nomura and A. H. MacDonald: Phys. Rev. Lett. **96** (2006) 256602.
- 30) B.G. Frederisk, G. Apai, and T. N. Rhodin: Phys. Rev. B **44** (1991) 1880.
- 31) S. Desgreniers and K. Lagarec: Phys. Rev. B **59** (1991) 8467.
- 32) L. Kang, B. H. Lee, W.-J. Qi, Y. Jeon, R. Nieh, S. Gopalan, and J. C. Lee: IEEE Electron Device Lett. **21** (2000) 181.
- 33) T. Ando: J. Phys. Soc. Jpn. **75** (2006) 054701.